⌘ *Author's Choice*

THE JOURNAL OF BIOLOGICAL CHEMISTRY VOL. 284, NO. 23, pp. 15564–15572, June 5, 2009

Angiotensin-converting Enzyme Is a Modifier of Hypertensive End Organ Damage*[S]

Received for publication, August 25, 2008, and in revised form, March 6, 2009 Published, JBC Papers in Press, March 23, 2009, DOI 10.1074/jbc.M806584200

Xiaojun Liu[‡], Christopher O. C. Bellamy[§], Matthew A. Bailey[‡1,2], Linda J. Mullins[‡1], Donald R. Dunbar[‡2], Christopher J. Kenyon[‡], Gillian Brooker[‡], Surasak Kantachuvesiri[¶], Klio Maratou[‖], Ali Ashek[‡], Allan F. Clark[‡], Stewart Fleming[**], and John J. Mullins[‡3]

*From the [‡]Molecular Physiology Laboratory, Centre for Cardiovascular Science, Queen's Medical Research Institute, University of Edinburgh, Edinburgh EH16 4TJ, United Kingdom, the [§]Pathology Department, Edinburgh Royal Infirmary, Edinburgh EH16 4SA, United Kingdom, [¶]Mahidol University, Bangkok 10400, Thailand, the [‖]Medical Research Council Clinical Sciences Centre, Hammersmith Hospital, London W12 ONN, United Kingdom, and **Ninewells Hospital, Dundee DD1 9SY, United Kingdom*

Severe forms of hypertension are characterized by high blood pressure combined with end organ damage. Through the development and refinement of a transgenic rat model of malignant hypertension incorporating the mouse renin gene, we previously identified a quantitative trait locus on chromosome 10, which affects malignant hypertension severity and morbidity. We next generated an inducible malignant hypertensive model where the timing, severity, and duration of hypertension was placed under the control of the researcher, allowing development of and recovery from end organ damage to be investigated. We have now generated novel consomic Lewis and Fischer rat strains with inducible hypertension and additional strains that are reciprocally congenic for the refined chromosome 10 quantitative trait locus. We have captured a modifier of end organ damage within the congenic region and, using a range of bioinformatic, biochemical and molecular biological techniques, have identified angiotensin-converting enzyme as the modifier of hypertension-induced tissue microvascular injury. Reciprocal differences between angiotensin-converting enzyme and the anti-inflammatory tetrapeptide, *N*-acetyl-Ser-Asp-Lys-Pro in the kidney, a tissue susceptible to end organ damage, suggest a mechanism for the amelioration of hypertension-dependent damage.

Malignant hypertension (MH)[4] is a complex trait with both genetic and environmental factors affecting development and prognosis. Although improved diagnosis and preventative medication has greatly reduced the incidence of MH (1–3), the predisposing factors that trigger its onset are poorly understood (4, 5). To gain insight into its genetic basis, we previously generated a transgenic MH rat model, TGR(mRen2)27 (6), in which the mouse *Ren2* renin gene, driven by its endogenous promoter, was incorporated into the Hanover Sprague-Dawley rat (extensively reviewed; see Refs. 5 and 7–13). However, the spontaneous and rapid (24–48 h) development of MH between 50 and 90 days of age and heterogeneity of the outbred Sprague-Dawley genetic background made the model unsuitable for molecular dissection. Using informative crosses with Fischer (F344) and Lewis (Lew) rat strains, the penetrance of and survival from MH was found to be genetically determined (14, 15). Resistance of the Lewis strain to the effects of highly elevated blood pressure, and malignant hypertension severity was shown to involve an unknown modifier located within the malignant hypertension severity quantitative trait locus (QTL) on chromosome 10 (15).

To refine the experimental strategy, we placed the mouse *Ren2* renin cDNA under the control of an inducible cytochrome P-450 1a1 (Cyp1a1) promoter, on the Fischer (F344) genetic background (Ren2.F), the transgene being integrated on the Y chromosome (16). Judicious induction with the nontoxic xenobiotic indole-3-carbinol (I3C) allowed the development of hypertension or transition to MH, the extent of end organ damage, and the repair processes to be analyzed in detail (5, 11, 16–25).

To determine whether the strain specific response to highly elevated blood pressure is due to the timing or extent of vascular damage, a consomic rat strain was derived in which the inducible transgene was maintained on the Lewis background. To investigate the contribution of the modifier of end organ damage (MOD) to strain differences, we also derived two congenic strains in which the reciprocal QTLs were introduced onto the consomic backgrounds. These newly developed lines were used to determine the genetic contributions of background strain and QTL to various parameters of blood pressure, renal function, and end organ damage. Using a wide range of techniques, including reverse transcription-PCR, Western blot, enzyme assay, and microarray analysis, angiotensin-converting enzyme has been identified as a modifier of end organ damage.

* This work was supported by a Kidney Research UK (formerly National Kidney Research Fund) award (to J. M. and S. F.), Wellcome Trust Programme Grant WTO53646, the Wellcome Trust Cardiovascular Research and Functional Genomics initiatives, and the EURATools consortium.

⌘ *Author's Choice*—Final version full access.

[S] The on-line version of this article (available at http://www.jbc.org) contains supplemental Figs. S1–S4 and Tables S1–S3.

[1] Both authors contributed equally to this work.

[2] Recipients of Wellcome Trust Intermediate fellowships.

[3] Recipient of the Wellcome Trust Principal Fellowship. To whom correspondence should be addressed: Molecular Physiology Laboratory, CVS, QMRI, University of Edinburgh, 47, Little France Crescent, Edinburgh EH16 4TJ, UK. Tel.: 44-131-242-6722; Fax: 44-131-242-6782; E-mail: j.mullins@ed.ac.uk.

[4] The abbreviations used are: MH, malignant hypertension; Ace, angiotensin-converting enzyme; QTL, quantitative trait locus; BC, backcross; I3C, indole-3-carbinol; MOD, modifier of end organ damage; RPF, renal plasma flow; GFR, glomerular filtration rate; Ang, angiotensin; MABP, mean arterial blood pressure; Ac-SDKP, *N*-acetyl-Ser-Asp-Lys-Pro; ANOVA, analysis of variance.

EXPERIMENTAL PROCEDURES

Breeding Scheme for Generating Consomic and Congenic Strains—Derivation of the consomic strain Ren2.L was performed by a marker-assisted breeding program in which Ren2.F males (carrying the Ren2 transgene on the Y chromosome) were backcrossed with Lewis females. Progenitors of each generation were selected by microsatellite genotyping with 125 markers chosen at 10–15 cM to provide coverage of all autosomes.

Congenic strains, Ren2.F-MOD-L and Ren2.L-MOD-F, were also derived by a marker-assisted breeding program. In brief, Ren2.F males and Lewis females were bred to produce F1 rats. F1 males were backcrossed to either Lewis or F344 females to produce the first backcross generation BC1-Lew or BC1-F344, respectively. The males were genotyped for markers spaced approximately every 15 cM. The optimal BC1-Lew male rats, which were heterozygous F344/Lew for the MOD QTL region but possessed the maximum Lew/Lew homozygosity for the nonrelevant autosomal region of the genome, were selected and backcrossed to Lewis females to produce each subsequent backcross generation. From BC5, male progeny were genotyped only for markers spanning the MOD QTL region. After 12 backcross generations, males and females heterozygous for F344/Lew in the reduced MOD QTL region were brother-sister mated to generate the homozygous congenic strain Ren2.L-MOD-F, which carried the mouse Ren2 transgene on the Y chromosome, was homozygous F344/F344 for the MOD QTL region, but was homozygous Lew/Lew for the rest of the genome. Congenic strain Ren2.F-MOD-L was generated by repeated backcrossing to F344 females in an analogous manner to yield animals that were homozygous Lew/Lew for the MOD QTL region but homozygous F334/F344 for the rest of the genome (see Fig. 1*a*).

Treatment—The animal studies were undertaken under United Kingdom home office license, following review by local ethics committee. All of the rats were housed individually, given free access to water and standard commercial rat chow (Special Diet Services, Witham, Essex, UK), and maintained under controlled conditions of temperature (21 ± 1 °C) and humidity (50 ± 10%), under a 12-h light/dark cycle. Animals (12–14 weeks old) from each strain were randomly divided into three groups (8 rats/group). The animals from groups 1 and 2 were given 100 mg of I3C/kg of body weight/day by gastric gavage for 7 and 10 days, respectively. Control group 3 was gavaged with carrier (vegetable oil).

Blood Pressure—Direct blood pressure of six animals in each strain was monitored by radiotelemetry using surgically implanted transmitters (Data Sciences International, St. Paul, MN). The signal was decoded using Art 4.0 software, and systolic blood pressure, mean blood pressure, and diastolic blood pressure data were collected.

Blood and Tissue Collection—The blood samples were collected into potassium EDTA-coated microvette tubes for renin assays, 1.5-ml Eppendorf tubes for Ace activity measurement or heparinized tubes containing captopril at 10^{-5} M final concentration for measurement of *N*-acetyl-Ser-Asp-Lys-Pro (Ac-SDKP). The samples for renin and Ac-SDKP measurement were centrifuged at 4 °C for 6 min, and plasma was snap-frozen and stored at −70 °C prior to assay. The samples for Ace activity measurement were held for 2–3 h at room temperature and then centrifuged at 1000 × *g* for 10 min. The serum was collected and kept at −70 °C until use. At the end of the study, the animals were killed by CO_2 inhalation and cervical dislocation. Tissues including lung, left kidney, and liver were immediately frozen in dry ice and stored at −80° until use. Tissues including mesentery, heart, pancreas, and right kidney were fixed in 10% neutral buffered formalin for pathological examination and immunohistochemical analysis.

Plasma Renin Activity Determination—Plasma renin activity was measured by a modification of the method described previously (26). Aliquots of plasma were incubated at 0 and 37 °C for 30 min with angiotensin I (Ang I) antiserum (a generous gift of Dr J. J. Morton, University of Glasgow) in Tris buffer (pH 7.4, 50 mM). The Ang I generated and trapped was measured by radioimmunoassay. Plasma renin activity values are given as ng of Ang I·h^{-1}·ml^{-1}.

Renal Function Study—The animals were anesthetized (120 mg of inactin/kg intraperitoneally) and prepared for renal function studies as previously described (27). The rats were infused intravenously with a saline solution containing 0.5% *para*-amino hippuric acid and 0.5% fluorescein isothiocyanate-inulin for measurement of renal plasma flow (RPF) and glomerular filtration rate (GFR) respectively. After a 1-h equilibration period, urine was collected for 60 min, and blood (200 μl) was collected before and after. The concentration of *para*-amino hippuric acid and fluorescein isothiocyanate-inulin were measured in urine and plasma by colorimetry and fluorimetry, respectively.

Histological Examination and Immunohistochemical Analysis—Mesentery, pancreas, kidney, and heart were evaluated for microvascular changes using conventional hematoxylin and eosin and periodic acid-Schiff-stained 3-μm histologic sections. The sections were scored blind to the experimental group and time point. In the heart, necroinflammatory lesions were counted in sequential transverse sections comprising left ventricle, interventricular septum, and right ventricle. For other organs, the severity of arterial microvascular changes was evaluated on a 5-point ordered categorical scale for reactive myoadventitial changes (scoring 1 or 2 by severity and prevalence) and destructive mural lesions that are a hallmark lesion of malignant phase hypertension (scoring 3–5 according to prevalence; see supplemental Fig. S3). Myoadventitial expansion with mononuclear cells and myofibroblasts was associated with medial changes of myocyte enlargement, amphophilic cytoplasmic staining, nuclear enlargement, occasional mitoses, and, in the most severe examples, apparent myocyte disarray. Hallmark destructive changes were characterized by evidence of intramural contiguous cell death (necrosis) and/or fibrinoid change. For statistical evaluations the groups were compared nonparametrically, on the basis of the presence or absence of hallmark destructive vascular changes (score 3–5 inclusive), so error bars are inappropriate.

Immunohistochemistry for Ace protein used mouse anti-Ace monoclonal antibody (MAB3502; Chemicon International, 1:125 dilution). De-waxed and rehydrated paraffin sections (3

μm) underwent antigen retrieval in a microwaveable pressure cooker for 2.5 min at pressure before incubation with primary antibody solution for 30 min at room temperature. Bound antibody was labeled and visualized using the DAKO Envision + system horseradish peroxidase kit, before counterstaining sections with Mayer's hematoxylin. Negative control slides omitted the primary antibody.

Microarray Analysis—Gene expression profiles from kidney RNA of Ren2.F, Ren2.L, Ren2.F-MOD-L, and Ren2.L-MOD-F were analyzed at 0, 7, and 10 days after induction. Four biological replicates were used for each condition. The left kidneys were dissected, and both fat and kidney capsules were removed. The kidneys were quartered, transferred to 2-ml Eppendorf tubes, snap frozen in liquid nitrogen, and stored at −80 °C. Total RNA was extracted (TRIzol reagent; Invitrogen), purified (RNeasy Mini kit; Qiagen), and DNase I-treated (RNase-Free DNase Set; Qiagen), according to the manufacturers protocols. RNA concentration and purity was determined with a NanoDrop ND-1000 spectrophotometer (NanoDrop Technologies, Wilmington, DE) and Agilent 2100 Bioanalyser (Agilent Technologies, Santa Clara, CA). RNA samples were immediately frozen and stored (−80 °C). Biotin-labeled targets for the microarray experiment were prepared using 1 μg of total RNA. Ribosomal RNA was removed with the RiboMinus human/mouse transcriptome isolation kit (Invitrogen), and cDNA was synthesized using the GeneChip® whole transcript sense target labeling and control reagents kit (Affymetrix, Santa Clara, CA). 5 μg of biotinylated target was hybridized with the GeneChip® rat exon 1.0 ST array (Affymetrix) at 45 °C for 16 h. After washing, specifically bound target was detected using the GeneChip hybridization, wash and stain kit, and the GeneChip Fluidics Station 450 (Affymetrix). The arrays were scanned using the GeneChip Scanner 3000 7G (Affymetrix), and CEL intensity files were produced using GeneChip operating software version 1.4 (Affymetrix). CEL files were analyzed in Bioconductor using the OneChannelGUI package. Robust multi-array average sketch was used to generate probe summaries using the extended probe set for the gene and exon level. Limma was used to generate raw p values, and the Benjamini and Hochberg procedure was used for multiple testing corrections. Genes with a corrected p value less than 0.05 were classed as differentially expressed.

Bioinformatics Analyses—The Ensembl (28) data base (release 46) was mined with the BioMart tool to identify genes in the MOD locus. The positions of markers D10Rat15 and D10Rat142 were used to limit a search on rat chromosome 10. Gene identifiers, symbols, descriptions, and ontology information were extracted to help identify genes of interest. The name and symbol of each gene were concatenated to generate a gene query string (for example, "Mapt or microtubule-associated protein tau"). These strings were used to query the Pubmed data base via Pubmatrix (29) for co-citation with relevant terms (including hypertension, kidney, renal, vasculature, and pathology). In addition, gene expression profiles were inferred by using data from Unigene, Gene Expression Omnibus, and Array Express as appropriate.

Quantitative Real Time PCR—Total RNA was extracted from tissues using TRIzol reagent (Invitrogen). The RNA was treated with DNA-Free (Ambio, Austin TX) and quantified, and its integrity confirmed by gel electrophoresis. RNA (3 μg) was reverse transcribed, using a SuperScript II first strand cDNA synthesis kit (Invitrogen). The resultant cDNA was amplified by TaqMan real time quantitative PCR on either the ABI Prism 7000 sequence detection system (Applied Biosystems, Warrington, UK) or the LightCycler 480 real time PCR system (Roche Applied Science). (The PCR primers are given in supplemental Table S3.) The reactions were carried out in triplicate and normalized to 18 S for the samples from kidney and wbscr1 for samples from liver.

Western Blot—The kidney samples were homogenized, and proteins were extracted for Western blot analysis exactly as described (30).

Ace Activity Assay—Serum Ace activity was measured using a commercial kit (Alpha Laboratories, Eastleigh, UK) adapted for use on the Cobas Fara Centrifugal analyzer (Roche Applied Science). The *in vivo* activity of Ace was tested in cohorts of non-induced Ren2.L ($n = 5$) and Ren2.F ($n = 5$) rats by measuring the pressor response to bolus injections of Ang I (2.5, 5, 10, 20, 40, and 80 ng). The peptide was injected in 0.1 ml of saline at 10–15-min intervals; injection of saline alone had no effect on MABP. Pressor responses to Ang I were abolished by prior injection of captopril (3 mg/kg), thereby confirming Ace as the principal route of acute angiotensin II generation.

Tissue Ace Activity and K_m Determination—Tissue Ace activity was assayed by an adaptation of the method of Santos *et al.* (31), replacing serum with tissue, homogenized in ice-cold lysis buffer (30 mM KCl, 0.25 M sucrose, 1% Triton X-100), and spun to remove cell debris (500 × g; 15 min; 4 °C), utilizing the tripeptide Hip-His-Leu (Sigma) as substrate. Fluorescence (excitation, 355 nm; emission, 460 nm) of the dipeptide product was measured in duplicate samples using a 1420 Multilabel HTS counter (PerkinElmer Life Sciences) and adjusted according to protein concentration. Ace activity is expressed as mM His-Leu/g of protein/h at 37 °C.

For K_m determination, 1 μl of lung extract was incubated with various concentrations of Hip-His-Leu substrate (0.1, 0.2, 0.3, 0.5, 0.75, 1.0, 1.25, 1.5, 2, 4, and 5 mM) for 15 min, respectively. The hydrolysis of Hip-His-Leu was measured by fluorimetry as described above. The K_m was calculated by nonlinear regression analysis (using Graphpad Prism).

Plasma and Tissue Ac-SDKP Measurement—Ac-SDKP concentration was measured after cold methanol extraction of plasma or tissue homogenate (32) by a competitive enzyme immunoassay (Spi Bio, Massy, France) according to the manufacturer's protocol. The results are presented as pmol Ac-SDKP/mg extracted protein (as determined by BCA protein assay kit; Pierce).

Statistical Analysis—The measurement data are summarized with the means ± S.E. Statistical comparison of means was made using t test or ANOVA followed by Bonferroni's post hoc test. The ordered categorical pathologic scores of tissue microvascular injury were analyzed with Fisher's exact probability test (one tailed) or with Chi square tests, comparing for the presence or not of destructive vascular lesions. $p < 0.05$ was judged to indicate significance.

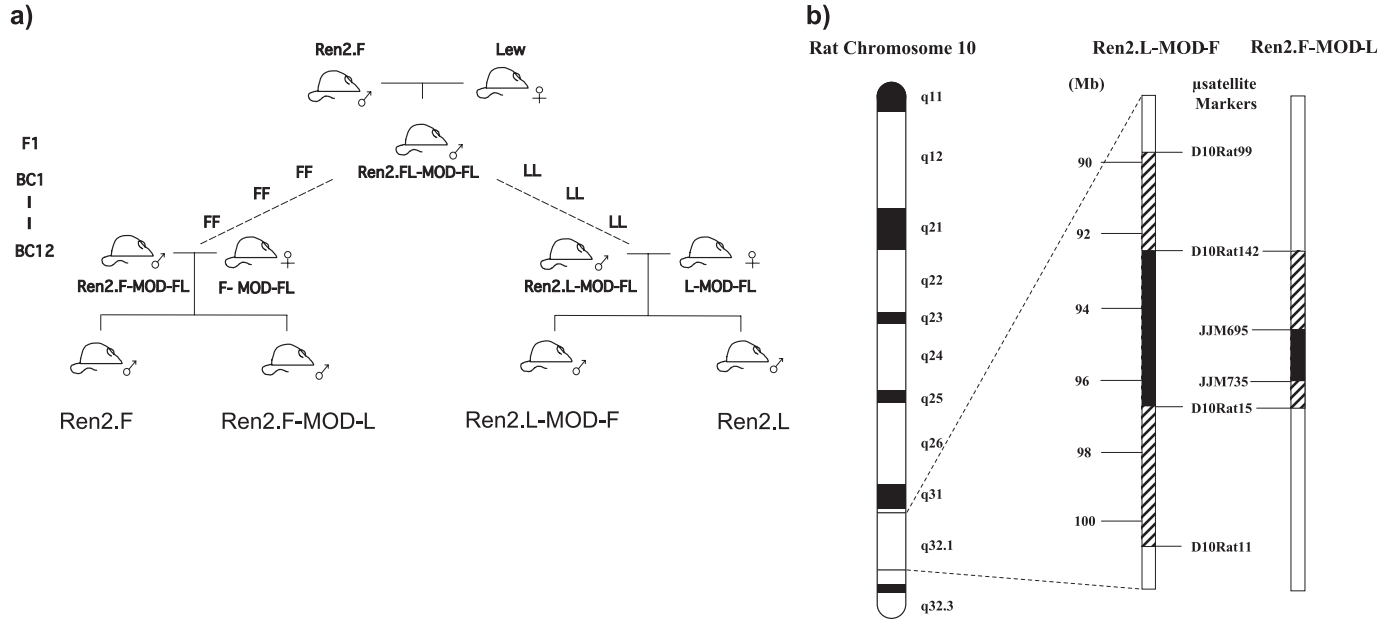

FIGURE 1. **Production of the congenic strains and mapping of the MOD QTL.** *a*, Ren2.F males and Lewis females were bred to produce F1 animals. F1 males were backcrossed to Lewis or F344 females, respectively, for 12 generations, the choice of male at each generation being marker-assisted. Brother-sister matings produced Ren2F-MOD-L and Ren2L-MOD-F strains. *b*, the extent of the congenic region on chromosome 10 (*hatched box*) was determined using informative microsatellites and further refined (*black box*) by scanning informative single nucleotide polymorphisms with high resolution melting analysis.

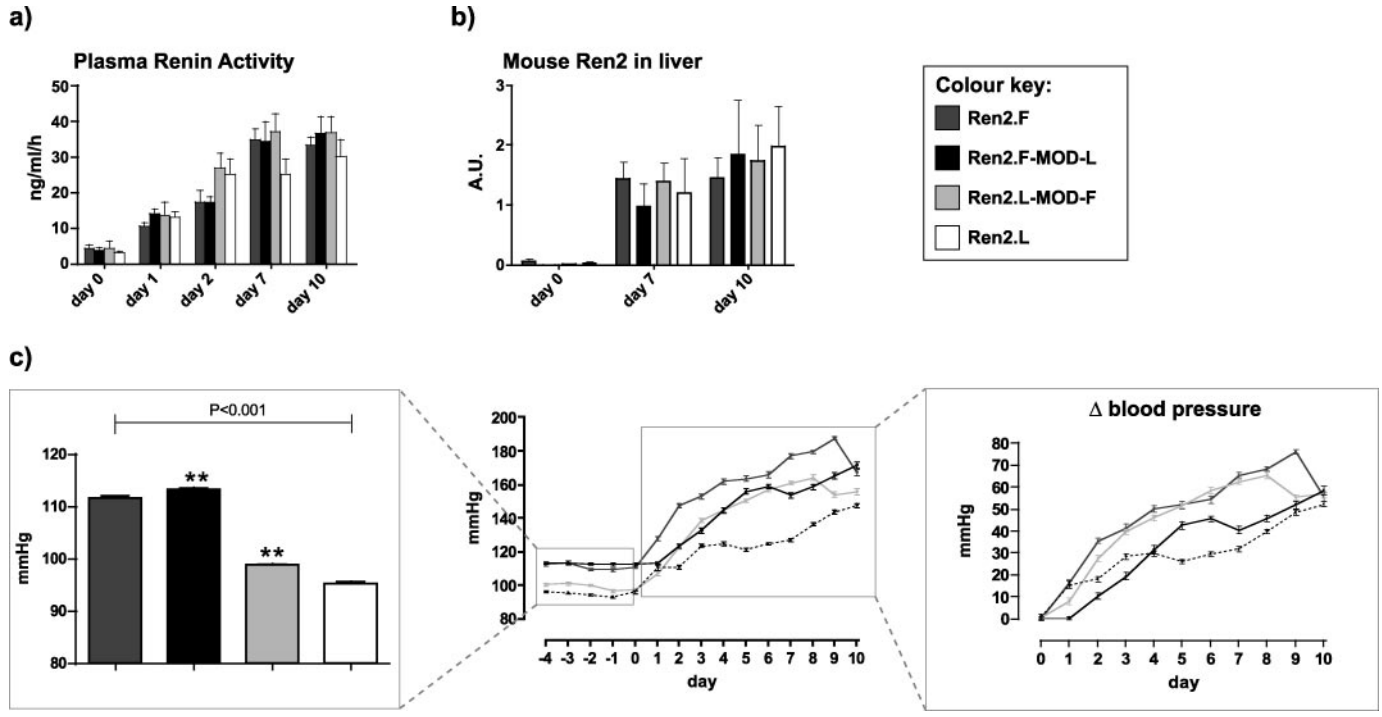

FIGURE 2. **Transgene expression in consomic and congenic lines before and after induction, and telemetric analysis of mean arterial blood pressure (n = 6/group/experiment).** *a*, plasma active renin. *b*, mouse Ren2 expression in the liver, relative to wsbcr1 expression. *c*, central panel shows the daily mean arterial blood pressures for 5 days prior to induction and for the 10-day duration of induction. *Left panel*, variation in MABP between strains prior to induction. *Right panel*, change in MABP during induction. **, $p < 0.01$ *versus* parental consomic. Ren2.L is shown as a *dotted line*, and the other groups are marked as per the key.

RESULTS

Development of Consomic and Congenic Strains—The strategy by which the Y chromosome-linked inducible renin transgene was introduced onto the Lewis (L) genetic background (Ren2L) is outlined in Fig. 1*a*. Development of the congenic strains, Ren2.F-MOD-L, in which a greatly reduced Lewis QTL is present on the F344 background, and Ren2.L-MOD-F incorporating the reciprocal QTL region, is also shown (Fig. 1*a*). The extent of each congenic region was ascertained using microsatellites (Fig. 1*b*). The maximum limit of the smaller congenic region (in Ren2F-MOD-L) was found to be ~4.0 Mb. A survey of informative single nucleotide polymorphisms within the QTL failed to reduce this region further (data not shown).

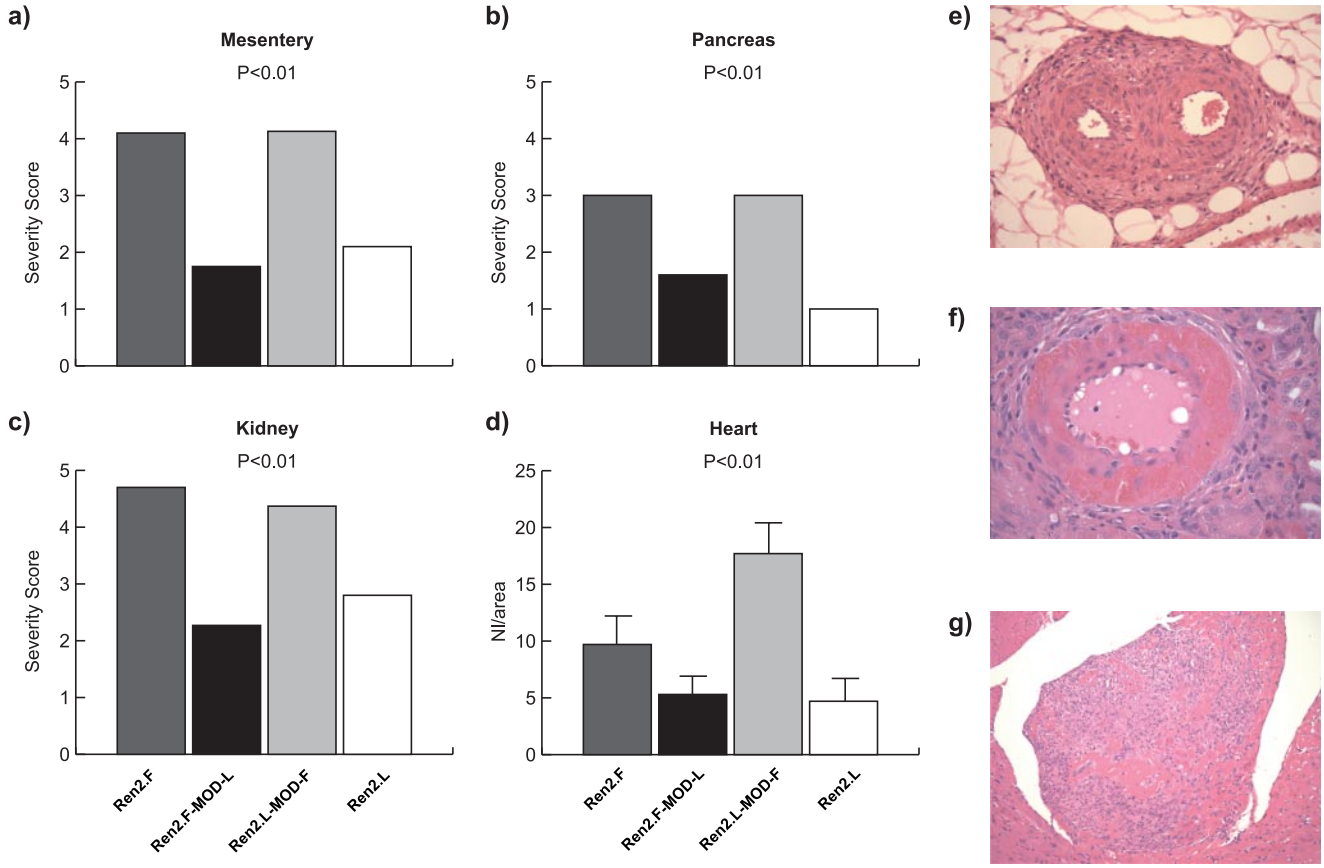

FIGURE 3. Pathological assessment of strains after induction in mesentery (*a*), pancreas (*b*), and kidney (*c*) is shown. The severity of microvascular injury was estimated with a 5-point ordered categorical scale according to the presence of reactive myoadventitial changes only (scoring 1 or 2 if widespread and severe) or additional destructive lesions, characterized by intramural necrosis and/or fibrinoid change (scoring 3–5 for a single focus, 2–3 foci, or >3 foci/section, respectively). In the heart (*d*), severity was the mean count of necroinflammatory lesions (*Nl*) in interventricular septum, left and right ventricle per cardiac transverse section. *e*, mesentery: small artery showing reactive myoadventitial changes: plump reactive medial myocytes and disarray, merging with adventitial proliferation and mononuclear inflammatory cell infiltration (approximate magnification, ×40). *f*, kidney: small artery showing a destructive lesion. There is mild adventitial proliferation and mononuclear cell infiltration surrounding a media with coagulative necrosis, intramural hemorrhage, and luminal endothelial hypertrophy (×60). *g*, heart, showing a necroinflammatory lesion affecting a right ventricular papillary muscle, with central coagulative necrosis, a surrounding mononuclear cell infiltrate and myofibroblastic proliferation (×20).

Transgene-derived and Endogenous Renin Expression—Plasma active renin levels were similar in the four rat strains prior to induction and, importantly, were increased by equivalent amounts throughout induction (Fig. 2*a*). There was no mouse renin mRNA detectable in the liver prior to induction (by reverse transcription-PCR analysis), but there was strong induction at day 7 and 10, with no statistical difference between strains at any time point (Fig. 2*b*). Endogenous rat renin levels in the kidney were suppressed by induction of the transgene (supplemental Fig. S1).

Effect of I3C Induction on MABP—The MABP of all strains was monitored before and during induction, and daily averages are presented (Fig. 2*c*, *central panel*). (For systolic and diastolic data see supplemental Fig. S2.) Prior to induction the MABP was significantly higher in Ren2.F and Ren2F-MOD-L than in Ren2.L and Ren2L-MOD-F, respectively (Fig. 2*c*, *left panel*), indicating that the background genotype rather than that of the congenic QTL region largely determines basal blood pressure. After transgene induction, blood pressure increased in all groups of rats (Fig. 2*c*, *central panel*; effect of induction $p < 0.001$; 2-way ANOVA), which was again influenced by genotype (Interaction $p < 0.001$). The increase in MABP was significantly greater in Ren2.F than Ren2.L with congenic strains achieving levels intermediate between the two consomic strains. Because preinduction blood pressures were not equivalent, the ΔMABPs following induction were compared (Fig. 2*c*, *right panel*). This analysis revealed that the MOD QTL, rather than background genotype, determines the hypertensive response to transgene induction. The fall in blood pressure in Ren2.F animals at day 10 may reflect onset of renal/heart failure as suggested by histological examination (see below).

Effect of I3C Induction on Body Weight—The Ren2.F and Ren2.L-MOD-F animals showed clinical signs of severe hypertension, including weight loss, by day 3, and their condition deteriorated over the induction period (with average weight loss of 10% after 7 days; data not shown). However the Ren2.L and Ren2.F-MOD-L animals showed no obvious clinical signs of severe hypertension under the same induction. This suggests that the propensity toward severe hypertension segregates with the MOD QTL.

Effect of I3C Induction on Tissue Pathology—Pathologic changes in the heart (necroinflammatory lesions) were counted, and changes in the microvasculature of kidney, mesentery, and pancreas were scored for the prevalence and degree

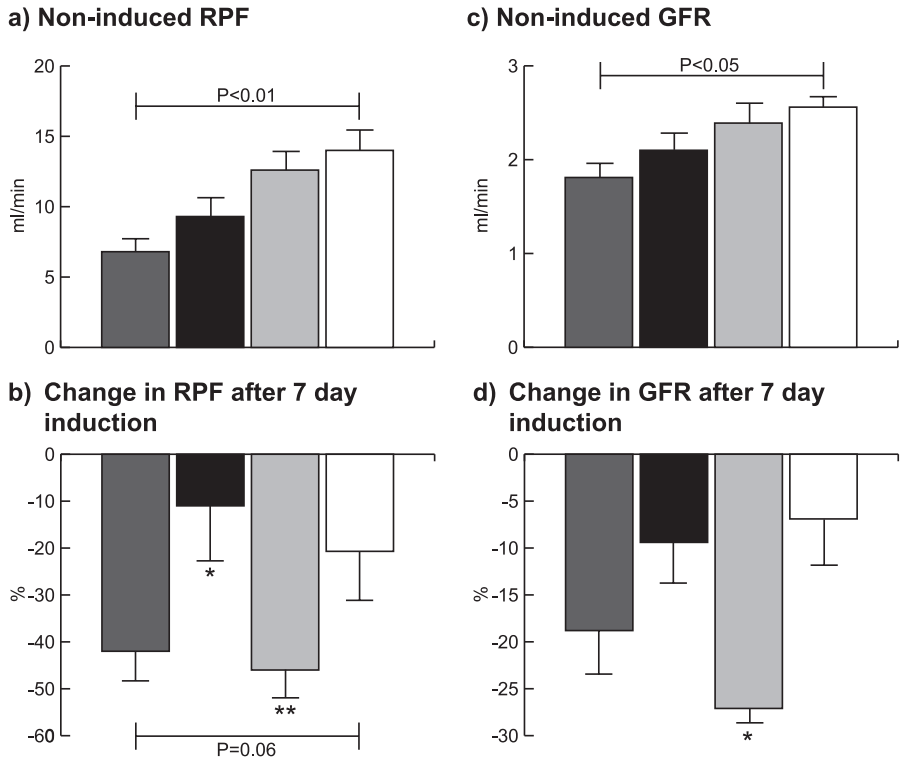

FIGURE 4. Renal hemodynamics were assessed before and following 7-day induction, by measuring renal clearance of *para*-amino hippuric acid and fluorescein isothiocyanate-inulin ($n = 6$/group/experiment) noninduced RPF (*a*), ΔRPF after 7 days induction (*b*), noninduced GFR (*c*), and ΔGFR after 7 days induction (*d*). *, $p < 0.05$; **, $p < 0.01$ *versus* parental consomic. *Dark gray*, Ren2.F; *black*, Ren2F-MOD-L; *light gray*, Ren2.L-MOD-F; *white*, Ren2.L).

of reactive myo-adventitial changes and destructive mural lesions characteristic of malignant hypertension. Typical histological sections are shown, and the scoring is summarized graphically (Fig. 3; see also supplemental Fig. S3 for additional histological sections and detailed description of pathology scoring). Despite evidence of pancreatic damage, the Ren2.L consomics and Ren2.F-MOD-L congenics showed the mildest effects of microvascular damage after transgene induction. The presence of hallmark destructive microvascular lesions in the different tissues correlated significantly with genotype at the MOD QTL and suggested that by 10 days of induction, the most severely affected Ren2.L-MOD-F and Ren2.F animals might be suffering heart failure (as evidenced by the fall in blood pressure). The pathologic changes were not simply a function of the absolute level of hypertension, because the tissue pathology in Ren2.L-MOD-F was more severe than that in the reciprocal congenic Ren2.F-MOD-L (mesentery, 7 days, $p = 0.0039$; kidney, 7 days, $p = 0.017$; and heart, 10 days, $p < 0.01$), despite similarly induced blood pressures. It is possible that the larger ΔMABP (in the Ren2.L-MOD-F group) from a lower base line may determine the subsequent severity of the MH pathology. (Earlier evidence (15) suggests that carrying Fischer genes at the chromosome 10 QTL in conjunction with Lewis genes at a second QTL on chromosome 17 (LOD3.9) had a multiplicative detrimental effect on mortality in TGR(mRen2)27 rats. It is possible that the chromosome 17 QTL contributes to severity of end organ damage in the Ren2.L-MOD-F consomic strain.)

Effect of I3C Induction on Renal Hemodynamics—Hypertensive end organ damage is characterized by renal vasoconstriction that contributes to ischemia and ultimately organ failure. Under noninduced conditions, there was a significant effect of background genotype on base-line renal hemodynamics; both RPF (Fig. 4*a*; $p < 0.001$; ANOVA) and GFR (Fig. 4*c*; $p < 0.05$ ANOVA) were lower in Ren2.F than Ren2.L. These differences were not determined by the MOD locus, because neither congenic was different from its parental strain. However, the degree of reduction in RPF that occurred after induction of hypertension corresponded to MOD QTL rather than background genotype (Fig. 4*b*). Qualitatively, the same genotype-phenotype relationships were also evident for GFR (Fig. 4*d*), but the effect of transgene induction appeared muted, possibly because of autoregulation of kidney filtration processes.

Microarray and PCR Analysis of Genes in QTL—Because Ren2.F-MOD-L exhibited ameliorated phenotype compared with Ren2.F, the MOD QTL region of 4.2 Mb must still retain the gene(s) responsible for the strain difference. Genome searches using Ensembl (RGSC 3.4, Dec 2004 genome build) revealed that the QTL spans 64 genes: 48 known genes (the best annotation status in Ensembl where each gene has a full-length cDNA for that species)/four "known by projection" genes/six predicted (all short noncoding RNA genes)/six novel genes. Microarray analysis allowed us to compare expression patterns of 43 of these genes, which were represented by good transcript clusters on the rat exon array in the extended probe set. (Sixteen other genes were represented by ambiguous transcript clusters, and five genes had no probes; see supplemental Table S1.) Of the 43 genes, only Ace was significantly differentially expressed in a QTL-dependent fashion. By literature mining for co-citation with relevant terms of interest (including hypertension, kidney, renal, vasculature, and pathology) and consideration of gene expression profiles (where known), we independently identified 17 genes as potential candidate genes within the QTL (Fig. 5*a*), and these genes were assessed by reverse transcription-PCR. Although some were differentially expressed on the basis of background genotype (supplemental Table S2), most showed no difference between strains. Only kidney *Ace* expression clearly followed the MOD QTL, a difference that was maintained during induction (Fig. 5*b*).

Characterization of Ace—Serum Ace activity (Fig. 6*a*) and Western blot analysis (Fig. 6*b*) revealed that both Ace activity and Ace protein are lower in noninduced Ren2.L than Ren2.F. Likewise, *in vivo* assessment of Ace function demonstrated significantly lower activity ($p < 0.001$; ANOVA) in Ren2.L rats

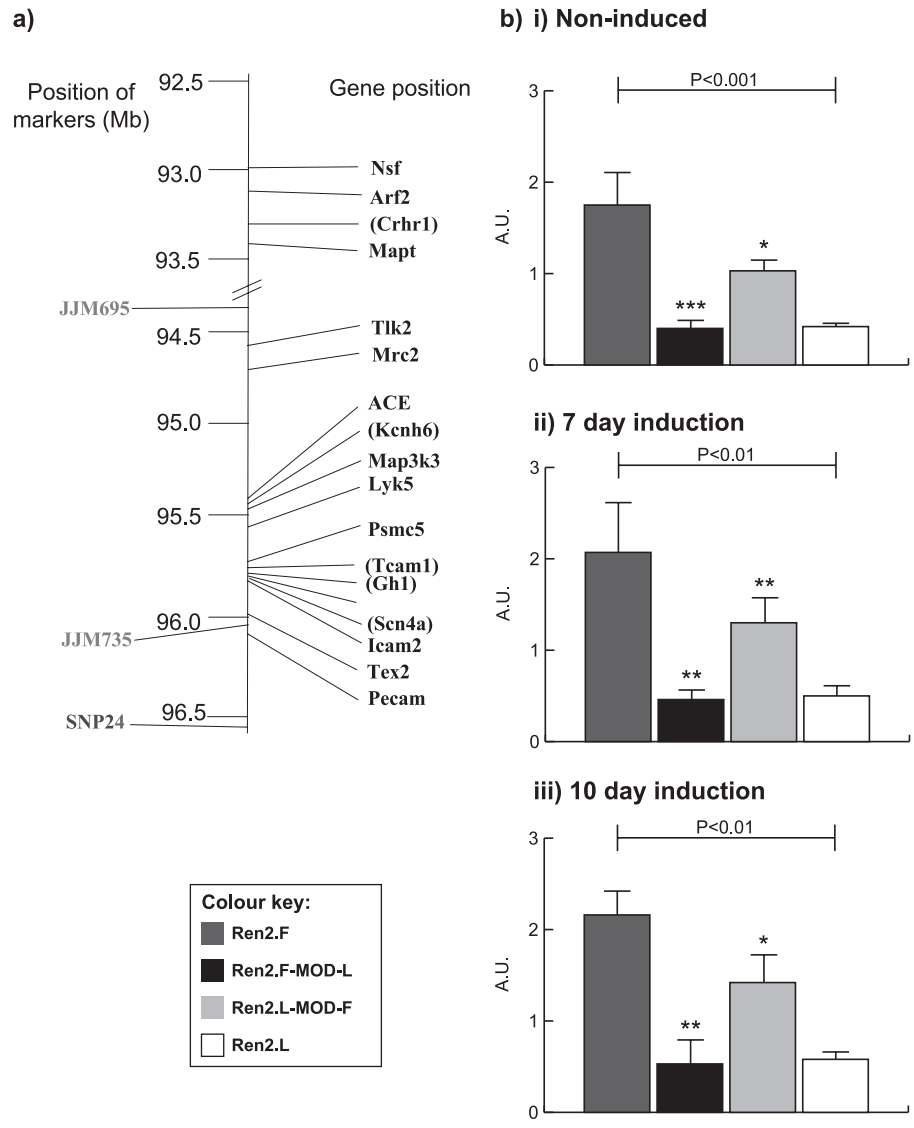

FIGURE 5. *a*, candidate genes, lying within or just outside the congenic region defined in Ren2.F-MOD-L. *b*, Ace mRNA expression in consomic and congenic strains (expressed as arbitrary units relative to 18 S) in noninduced kidney (*panel i*) and following 7 (*panel ii*) or 10 days induction (*panel iii*). *, $p < 0.05$; **, $p < 0.01$; ***, $p < 0.001$ *versus* parental consomic ($n = 6$).

than in Ren2.F (Fig. 6*c*). The similarity of EC_{50} of the two activity curves (Fig. 6*c*) suggests that the intrinsic catalytic activities are comparable, and the K_m of kidney Ace was found to be equivalent in Ren2.F and Ren2.L, using a synthetic substrate (1.139 ± 0.112 *versus* 1.055 ± 0.144 mM; $p < 0.002$). Immunohistological examination could not resolve differences in endothelial staining for Ace in target tissues between the consomic and congenic strains.

Characterization of Ac-SDKP—It has been shown that the N-terminal domain of Ace is able to cleave Ac-SDKP (33, 34), a naturally occurring tetrapeptide recently found to prevent and reverse inflammation, cell proliferation, and fibrosis in various rat models of hypertension (35, 36). Although neither plasma nor lung tetrapeptide levels differed between Fischer and Lewis animals (plasma, 2.61 ± 0.23 *versus* 2.28 ± 0.27, $p = 0.34$; lung, 6.73 ± 0.55 *versus* 5.23 ± 1.32, $p = 0.27$), kidney levels of Ac-SDKP were found to be significantly lower in Fischer than Lewis animals (8.27 ± 0.34 *versus* 9.98 ± 0.35, $p = 0.005$).

DISCUSSION

The analysis of consomic and congenic lines clearly shows that the degree of hypertension and severity of pathophysiological changes in MH is modified by gene(s) within the chromosome 10 QTL. Given the ambiguity of transcript clusters and the lack of probe sets, it is not technically possible to assay all 64 genes across the QTL by the currently available microarrays. We therefore used literature mining and expression profiles to independently identify possible candidate genes. These independent processes converged on *Ace* as the modifier gene responsible. We cannot exclude the possibility that an additional gene or genes within the QTL may contribute to the effect. To unequivocally confirm Ace as the sole modifier, it would be necessary to convert Fischer *Ace* to Lewis *Ace* by gene targeting, but this is not readily achievable in the rat as yet.

Ace is a powerful regulator of vascular function in multiple tissues, and evidence from widely different sources supports our results. Inhibition of the renin-angiotensin-aldosterone system in hypertension is clinically beneficial, yet the reduction in cardiovascular morbidity and remodeling is independent of the antihypertensive effect (37). Increased mouse *Ace* gene copy number does not affect blood pressure *per se* but exacerbates hypertension caused by additional environmental or genetic factors (38). In human population association studies, the genotype of *ACE* has been shown to predispose individuals to MH (39, 40). Treatment of TGR(mRen27) rats with subhypotensive levels of the Ace inhibitor ramipril specifically reduced tissue Ace and prevented the development of end organ damage (41) despite the increase in blood pressure associated with chronic expression of the transgene. This strongly implicated Ace or Ang II in the pathophysiological development of MH.

Previous studies on Ren2.F demonstrate that RPF decreases following I3C induction and that plasma and intrarenal Ang II levels increase (despite reduced levels of endogenous renal renin). All of these effects are prevented by the administration of the angiotensin II receptor type 1 receptor antagonist candesartan (21). Mineralocorticoid receptor blockade by spironolactone alleviates proteinuria following I3C induction but has

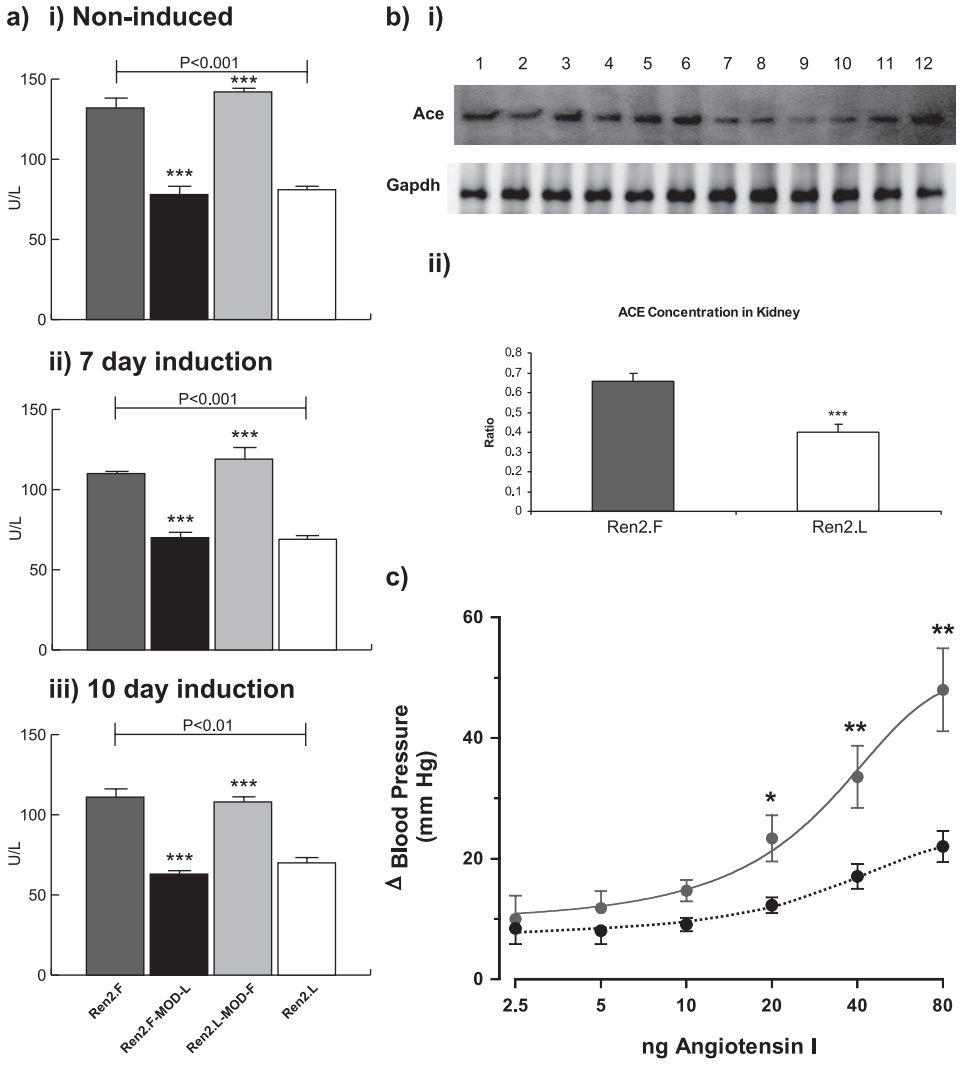

FIGURE 6. *a*, serum Ace activity in noninduced animals (*panel i*) or following 7 (*panel ii*) or 10 days induction (*panel iii*). *, $p < 0.05$; **, $p < 0.01$; ***, $p < 0.001$ ($n = 6$). *b*, *panel i*, Western analysis shows the relative expression of ACE in kidney between Fischer (*tracks 1–6*) and Lewis (*tracks 7–12*) rats. The *upper panel* shows immunoblot using ACE antibody, and the *lower panel* shows glyceraldehyde-3-phosphate dehydrogenase loading control. *Panel ii*, protein quantification by densitometry. The ratio of the means ± S.E. is shown (***, $p < 0.001$). *c*, the dose-response pressor effect of angiotensin I in cohorts of noninduced Ren2.F (*gray line*; $n = 5$) and Ren2.L (*dotted line*; $n = 5$) rats. The values are the means ± S.E. *, $p < 0.05$; **, $p < 0.01$.

little effect on systolic blood pressure, suggesting that the elevated arterial blood pressure (but not necessarily end organ damage) is independent of aldosterone stimulation (23). The basal (uninduced) differences in RPF and BP between consomic and congenic strains indicate that renal vascular resistance is higher on the Fischer than Lewis background. Intrarenal renin-angiotensin-aldosterone levels will contribute to this, but the basal strain difference results from the integration of multiple vasoactive systems (42). A major determinant of renal hemodynamic function was previously identified on chromosome 1 (43). We have now shown that Ace affects RPF following induction of hypertension.

The increased Ace protein levels in Ren2.F compared with Ren2.L parallel increased renal mRNA levels in the prehypertensive state, the cause of which remains to be elucidated, but it could reflect differences in regulation of transcription (44) or feedback regulation. Comparison of Lewis and F344 cDNA sequence reveals three base changes in the coding region, two of which are conservative. The third causes an amino acid substitution (L341F) in the N-terminal domain, which, by comparison to a three-dimensional model of the human N-terminal domain (with a competitive inhibitor molecule bound) (45) (supplemental Fig. S4), lies at the hinge between two helices. Modeling suggests that amino acid substitution in this loop would have only a minor effect on overall three-dimensional structure (supplemental Fig. S4). Studies of mice with specific inactivation of either the N or C-terminal domain suggest that the C-terminal rather than the N-terminal domain plays a major role in normal blood pressure control (33, 46). This may be the reason why measurement of *in vivo* ACE activities (with endogenous Ang I substrate) and K_m analyses (using the synthetic tripeptide substrate) yielded comparable results between Lewis and Fischer samples.

The N-terminal domain of human Ace has been shown to specifically cleave the naturally occurring peptide, Ac-SDKP, whereas specific inactivation of the mouse Ace N-terminal domain causes an accumulation of Ac-SDKP in plasma and urine (33). The tetrapeptide has recently been shown to act directly on bone marrow stem cells and macrophages, inhibiting their differentiation, activation, and cytokine release (47). Interestingly, the levels of Ac-SDKP were found to be raised in the kidney (an end organ damage-susceptible tissue) in Lewis compared with Fischer animals but not in the relatively damage-resistant lung. The reciprocal nature of tissue Ace and Ac-SDKP levels in susceptible tissues of Fischer and Lewis strains may explain the moderation of end organ damage in the latter strain. Using the N-terminally specific tetrapeptide substrate, both Ace activity and catalytic properties have been reported to be identical in both Lewis and Fischer strains (48).

We hypothesize that reduced efficiency of Ac-SDKP cleavage caused by reduced levels of Ace *per se* may ameliorate end organ damage through the anti-inflammatory effects of increased levels of tissue-specific tetrapeptide. The identification of Ace as a modifier of ΔMABP, ΔRPF, and hypertensive end organ damage suggests that ACE levels should be a consideration in discerning susceptibility to essential hypertensive tissue damage and MH in humans.

Acknowledgments—We thank Nicola Wrobel, Ann Hedley, Dr. J. Manning, and Dr. Forbes Howie for technical assistance. We thank Dr. Matthew Sharp and Professor Tim Aitman for helpful discussions. We thank Laurence Game and the Medical Research Council Clinical Sciences Centre microarray center for assistance.

REFERENCES

1. Lip, G. Y., Beevers, M., and Beevers, D. G. (1995) *J. Hypertens.* **13,** 915–924
2. Lip, G. Y., Beevers, M., and Beevers, G. (1994) *J. Hypertens.* **12,** 1297–1305
3. Edmunds, E., Beevers, D. G., and Lip, G. Y. (2000) *J. Hum. Hypertens.* **14,** 159–161
4. Kincaid-Smith, P. (1981) *Aust. N. Z. J. Med.* **11**, 64–68
5. Collidge, T. A., Lammie, G. A., Fleming, S., and Mullins, J. J. (2004) *Prog. Biophys. Mol. Biol.* **84,** 301–319
6. Mullins, J. J., Peters, J., and Ganten, D. (1990) *Nature* **344,** 541–544
7. Langheinrich, M., Lee, M. A., Bohm, M., Pinto, Y. M., Ganten, D., and Paul, M. (1996) *Am. J. Hypertens.* **9,** 506–512
8. Lee, M. A., Bohm, M., Paul, M., Bader, M., Ganten, U., and Ganten, D. (1996) *Am. J. Physiol.* **270,** E919–E929
9. Bader, M., and Ganten, D. (1996) *Clin. Exp. Pharmacol. Physiol.* **3,** (suppl.) S81–S87
10. Engler, S., Paul, M., and Pinto, Y. M. (1998) *Regul. Pept.* **77,** 3–8
11. Fleming, S. (2000) *J. Pathol.* **192,** 135–139
12. Wei, Y., Whaley-Connell, A. T., Chen, K., Habibi, J., Uptergrove, G. M., Clark, S. E., Stump, C. S., Ferrario, C. M., and Sowers, J. R. (2007) *Hypertension* **50,** 384–391
13. Whaley-Connell, A., Govindarajan, G., Habibi, J., Hayden, M. R., Cooper, S. A., Wei, Y., Ma, L., Qazi, M., Link, D., Karuparthi, P. R., Stump, C., Ferrario, C., and Sowers, J. R. (2007) *Am. J. Physiol.* **293,** E355–E363
14. Whitworth, C. E., Fleming, S., Cumming, A. D., Morton, J. J., Burns, N. J., Williams, B. C., and Mullins, J. J. (1994) *Kidney Int.* **46,** 1528–1532
15. Kantachuvesiri, S., Haley, C. S., Fleming, S., Kurian, K., Whitworth, C. E., Wenham, P., Kotelevtsev, Y., and Mullins, J. J. (1999) *Kidney Int.* **56,** 414–420
16. Kantachuvesiri, S., Fleming, S., Peters, J., Peters, B., Brooker, G., Lammie, A. G., McGrath, I., Kotelevtsev, Y., and Mullins, J. J. (2001) *J. Biol. Chem.* **276,** 36727–36733
17. Howard, L. L., Patterson, M. E., Mullins, J. J., and Mitchell, K. D. (2005) *Am. J. Physiol.* **288,** F810–F815
18. Mitchell, K. D., and Mullins, J. J. (2005) *Am. J. Physiol.* **289,** F1210–F1216
19. Patterson, M. E., Mouton, C. R., Mullins, J. J., and Mitchell, K. D. (2005) *Am. J. Physiol.* **289,** F754–F759
20. Opay, A. L., Mouton, C. R., Mullins, J. J., and Mitchell, K. D. (2006) *Am. J. Physiol.* **291,** F612–F618
21. Mitchell, K. D., Bagatell, S. J., Miller, C. S., Mouton, C. R., Seth, D. M., and Mullins, J. J. (2006) *J. Renin. Angiotensin Aldosterone Syst.* **7,** 74–86
22. Graciano, M. L., Mouton, C. R., Patterson, M. E., Seth, D. M., Mullins, J. J., and Mitchell, K. D. (2007) *Am. J. Physiol.* **292,** F1858–F1866
23. Ortiz, R. M., Graciano, M. L., Mullins, J. J., and Mitchell, K. D. (2007) *Am. J. Physiol. Renal Physiol.* **293,** F1584–1591
24. Patterson, M. E., Mullins, J. J., and Mitchell, K. D. (2008) *Am. J. Physiol.* **294,** F205–F211
25. Peters, B., Grisk, O., Becher, B., Wanka, H., Kuttler, B., Ludemann, J., Lorenz, G., Rettig, R., Mullins, J. J., and Peters, J. (2008) *J. Hypertens.* **26,** 102–109
26. Morton, J. J., and Wallace, E. C. (1983) *Clin. Sci.* (*Lond.*) **64,** 359–370
27. Bailey, M. A., Fletcher, R. M., Woodrow, D. F., Unwin, R. J., and Walter, S. J. (1998) *Am. J. Physiol.* **275,** F878–F884
28. Hubbard, T., Barker, D., Birney, E., Cameron, G., Chen, Y., Clark, L., Cox, T., Cuff, J., Curwen, V., Down, T., Durbin, R., Eyras, E., Gilbert, J., Hammond, M., Huminiecki, L., Kasprzyk, A., Lehvaslaiho, H., Lijnzaad, P., Melsopp, C., Mongin, E., Pettett, R., Pocock, M., Potter, S., Rust, A., Schmidt, E., Searle, S., Slater, G., Smith, J., Spooner, W., Stabenau, A., Stalker, J., Stupka, E., Ureta-Vidal, A., Vastrik, I., and Clamp, M. (2002) *Nucleic Acids Res.* **30,** 38–41
29. Becker, K. G., Hosack, D. A., Dennis, G., Jr., Lempicki, R. A., Bright, T. J., Cheadle, C., and Engel, J. (2003) *BMC Bioinformatics* **4,** 61
30. Tian, X. L., and Paul, M. (2003) *Biochem. Pharmacol.* **66,** 1037–1044
31. Santos, R. A., Krieger, E. M., and Greene, L. J. (1985) *Hypertension* **7,** 244–252
32. Cavasin, M. A., Liao, T. D., Yang, X. P., Yang, J. J., and Carretero, O. A. (2007) *Hypertension* **50,** 130–136
33. Fuchs, S., Xiao, H. D., Cole, J. M., Adams, J. W., Frenzel, K., Michaud, A., Zhao, H., Keshelava, G., Capecchi, M. R., Corvol, P., and Bernstein, K. E. (2004) *J. Biol. Chem.* **279,** 15946–15953
34. Rousseau, A., Michaud, A., Chauvet, M. T., Lenfant, M., and Corvol, P. (1995) *J. Biol. Chem.* **270,** 3656–3661
35. Rasoul, S., Carretero, O. A., Peng, H., Cavasin, M. A., Zhuo, J., Sanchez-Mendoza, A., Brigstock, D. R., and Rhaleb, N. E. (2004) *J. Hypertens.* **22,** 593–603
36. Peng, H., Carretero, O. A., Liao, T. D., Peterson, E. L., and Rhaleb, N. E. (2007) *Hypertension* **49,** 695–703
37. Pool, J. L. (2000) *Int. J. Clin. Pract.* **111,** (suppl.) 4–8
38. Krege, J. H., Kim, H. S., Moyer, J. S., Jennette, J. C., Peng, L., Hiller, S. K., and Smithies, O. (1997) *Hypertension* **29,** 150–157
39. Espinel, E., Tovar, J. L., Borrellas, J., Piera, L., Jardi, R., Frias, F. R., Armadans, L., and Bachs, A. G. (2005) *J. Clin. Hypertens.* (*Greenwich*) **7,** 11–17
40. Stefansson, B., Ricksten, A., Rymo, L., Aurell, M., and Herlitz, H. (2000) *Blood Press.* **9,** 104–109
41. Montgomery, H. E., Kiernan, L. A., Whitworth, C. E., Fleming, S., Unger, T., Gohlke, P., Mullins, J. J., and McEwan, J. R. (1998) *J. Hypertens.* **16,** 635–643
42. Evans, R. G., Eppel, G. A., Anderson, W. P., and Denton, K. M. (2004) *J. Hypertens.* **22,** 1439–1451
43. Iwai, N., Kinoshita, M., and Shimoike, H. (1999) *Circulation* **100,** 1923–1929
44. Challah, M., Villard, E., Philippe, M., Ribadeau-Dumas, A., Giraudeau, B., Janiak, P., Vilaine, J. P., Soubrier, F., and Michel, J. B. (1998) *Arterioscler. Thromb. Vasc. Biol.* **18,** 235–243
45. Natesh, R., Schwager, S. L., Sturrock, E. D., and Acharya, K. R. (2003) *Nature* **421,** 551–554
46. Fuchs, S., Xiao, H. D., Hubert, C., Michaud, A., Campbell, D. J., Adams, J. W., Capecchi, M. R., Corvol, P., and Bernstein, K. E. (2008) *Hypertension* **51,** 267–274
47. Sharma, U., Rhaleb, N. E., Pokharel, S., Harding, P., Rasoul, S., Peng, H., and Carretero, O. A. (2008) *Am. J. Physiol.* **294,** H1226–H1232
48. Jafarian-Tehrani, M., Listwak, S., Barrientos, R. M., Michaud, A., Corvol, P., and Sternberg, E. M. (2000) *Mol. Med.* **6,** 319–331